BNL-104673-2014-TECH

AGS/AD/Tech Note No. 250;BNL-104673-2014-IR

The 1985 Horizontal Survey

R. E. Thern

April 1986

Collider Accelerator Department

Brookhaven National Laboratory

U.S. Department of Energy

USDOE Office of Science (SC)

DISCLAIMER

Accelerator Division
Alternating Gradient Synchrotron Department
BROOKHAVEN NATIONAL LABORATORY
Associated Universities, Inc.
Upton, New York 11973

Accelerator Division
Technical Note

No. 250

The 1985 Horizontal Survey

R.E. Thern

April 28, 1986

TECHNICAL NOTE
The 1985 Horizontal Survey
Part I. Monuments

R. E. Thern
April 28, 1986

1. INTRODUCTION

During 1985 a partial survey of the radial position of the AGS magnets was done. The radial survey was interrupted to allow the crews to do a vertical realignment - there was not the time and manpower to do both before the AGS turn-on in the fall of 1985. This report shows what has been accomplished so far.

The primary reference for the radial position is the set of 24 control stations, or monuments, placed evenly around the ring, about 110 inches outside the beam line at each 10 foot straight section. These monuments are on 20 foot steel pipes isolated from the floor, but they have not proved to be stable over the long term either horizontally or vertically (1). The magnet stands are on the "pile caps", which are supported by four 50 foot piles and are also isolated from the floor. The pile caps may be more stable than the primary monuments, but they under the AGS ring and are poorly accessible, and do not have any horizontal survey references on them. (The pile caps do, however, have a vertical reference on them.)

The magnets themselves have survey sockets on top, near each end above the pole face centerline of the magnet. These sockets are measured with respect to the primary monuments to give the radial and azimuthal position of the magnet.

A series of horizontal surveys was done during the construction and early operation of the AGS, starting in 1958. The monuments and magnets were remeasured, and the magnets realigned, in 1962. This present survey is apparently the first complete (assuming that it will be completed) radial survey since then.

2. SURVEY

The primary monuments are evenly spaced around the ring on a 5165.4 inch (430.45') radius circle. The monuments are identified with one or two letters telling their position in the ring. For example, LA is near magnets L-20 and A-1, and A is near A-10 and A-11. One monument, FG, is obstructed by the SEB line, and a temporary monument, denoted FG', is used instead in the traverse to determine the monument locations. The permanent monument FG, which is needed for getting the magnet positions, is determined by angle and length from monument G.

The top of each monument consists of a disk with a bushed hole which is used to locate the survey instruments. After the initial survey, in 1958, the original disks were replaced by disks with holes offset to put them at the desired locations. Thus the monuments were all originally at their "ideal" positions on a regular 24-sided polygon (within survey errors), and any real differences from that now, or in the 1962 survey, must be due to monument motion.

For the initial surveys of the monuments, the magnets were not yet in place, and from each monument it was possible to sight to two adjacent monuments on each side. Thus there was a large degree of redundancy in the original measurements, with completely measured triangles, three angles and three sides, formed at each three consecutive monuments. Such redundancy is no longer possible, because with the magnets in place, only the immediately adjacent monuments are visible to each other. Thus the present monument survey consists only of the distances between adjacent monuments, and the angle at each vertex.

The angles were measured with a Wild T3 transit, taking five sets of readings, reading three crosshairs in each set, giving 15 measurements which are averaged. The surveyors expect an accuracy of .6-.7 seconds of arc; the manufacturer's literature claims a standard deviation of 0.5 second. The 15 independent measurements of each angle have an rms of typically about .6 sec; thus the average may be expected to have a standard deviation of $.6/\sqrt{15}$ or about .15 seconds, but claiming such accuracy does not appear to be warranted. All angles were later reduced by 0.3 sec to correct for a miscentering of the instrument (the ball which locates the instrument in the hole in the monument was not centered on the axis of the instrument). After this correction, the sum of the 24 angles differed from 360 degrees by 3.1 seconds, which is consistent with an rms error of $3.1/\sqrt{24} = 0.63$ seconds in each.

Although the survey group was prepared to measure the distances between monuments with a laser interferometer, there was not sufficient time to do this, so the distances were measured with an invar tape instead. One intermonument distance was measured with the interferometer, and this was used to calibrate the tape in the morning and afternoon of each of the four days for this job. These eight calibrations of the tape have an rms spread of .014", which is an order of magnitude larger than would be expected from the temperature variations. The average of these eight tape calibrations was then used to calculate the intermonument distances. Three of the distances (F-FG', FG'-G, and GH-H) were measured with a surveyors tape measure instead and are thus subject to larger errors.

In what follows, the random errors in angle and length are estimated to be

sigma-angle = 0.6 sec
sigma-length = 0.014 inch

except for the distances measured with the tape measure, which are estimated to have errors twice the above.

3. ANALYSIS

The 24-sided figure determined by a traverse around the ring, measuring angles and lengths, will in general not close on itself, and the measured quantities must be adjusted slightly to give a closed figure. A least squares fit should give the best (i.e., most probable) result. If the deviations from a perfectly symmetrical figure are small, the computation of the fit can be done in a relatively simple way (1,2), but in our case the symmetry is ruined by the use of the temporary monument instead of FG. A general least squares fit for a traverse like ours, which has a very low level of redundancy, is also quite simple, requiring only a three-by-three matrix equation. This is shown in Appendix A, along with a comparison with other methods of achieving closure.

Using a least squares fit should give fitted values which are closer to the true values than were the original measurements. However, the improvement

to be expected in a case like this, where the degree of overdetermination is small, is slight. With 48 measurements, we have for the expected value of the sum of errors squared (where the sum ranges over the 24 angles and 24 lengths)

$$\langle \Sigma (x_{true} - x_{measured})^2 / \sigma^2 \rangle = 48$$

where the true values, of course, are not known. After a fit with only three degrees of freedom, we have, for the sum of residuals squared,

$$\langle \Sigma (x_{fit} - x_{measured})^2 / \sigma^2 \rangle = 3$$

These fitted values still have errors with an expected value

$$\langle \Sigma (x_{true} - x_{fit})^2 / \sigma^2 \rangle = 48 - 3 = 45$$

which is not much better than the measured values. (This relationship is explained in Appendix A). The real virtue of the fitted values is that they describe a closed figure, without a discontinuity between the starting and ending points. As is shown in Appendix A, other methods of enforcing closure on the data give answers which are slightly "different" but probably not significantly "less correct".

4. RESULTS

After adjusting for angle closure, the monument data fails to close by 0.210 inches (dx=-.209, dy=.017). The least squares fit to close the figure gives a chisquare of 9.44, compared to an expected value of 3 for the number of degrees of freedom here. The discrepancy may be due to bad luck (2% confidence level), an underestimate of the random errors, or mistakes (blunders) in the data. Mistakes, if any, are most likely in the length data, since the angles were measured multiple times and averaged.

Table 1 gives the data, and Table 2 thefitted coordinates of the monuments, making the calculation to use permanent monument F6. Also shown are deviations of the monuments from their ideal positions, in both x-y and polar coordinates. The absolute coordinates of the monuments are not, of course, determined by this survey. The survey data only gives a 24-sided polygon, which must be oriented using some extra criteria. The coordinate system has been chosen here by translating and rotating the 24-sided polygon, so that the average of the deviations from the ideal monument positions in x, y, and azimuth are zero. (Or, to visualize it another way, the centroid of the 24 points is put at (0,0), and the figure rotated to make the points lie as close as possible to rays from the center at 15 degree multiples from 'east'). The average radial deviation of the points reflects a change in the "radius" of the monument figure. It is, of course, real, and can not be made zero by any choice of coordinate system. Figure 1 shows these radial deviations. The average radial position is 0.113" inside the original positions on the ideal figure. This much deviation could be due to a systematic undermeasurement of the intermonument lengths by

$$.113" \times 2\pi / 24 = .030"$$

Such a systematic effect, which would have to come from the tape calibration with the laser interferometer, is considered unlikely by the surveyors.

Also shown in Figure 1 are the radial deviations determined in the 1962 survey. The present deviations are larger by a factor of approximately four. Figure 2 shows the 1962 deviations magnified by a factor of four, compared with

the present. There is an indication that in the region of the ring away from the external lines, which have been extensively changed since 1962, the monument motion which occurred from 1960 to 1962 has continued and is now about four times as great. There are some caveats to this interpretation. Monuments FG, G, GH, H, and IJ were apparently given new offset disks after the 1962 survey so their motion started over from 'zero' again then. The monument at IJ showed a very large motion in the 1962 survey, presumably due to the removal of the adjacent wall for the construction of the conjunction area; it has behaved like its neighbors since then.

Figure 3 shows the x and y deviations for the present data, added to a figure from ref. 1 which gave results for the 1962 and older data. (Figure B12 shows the present deviations at a smaller scale and is perhaps less confusing). The present deviations are substantially larger than before. It should be remembered that the absolute origin is arbitrary for each survey. Thus the motion of a single monument (or one measuring mistake) will cause an apparent motion of all monuments.

Since the radial survey of the magnets depends on the monument survey, it is crucial that the monuments be correct. The present data give a disconcertingly high chisquare, suggestive of a possible blunder somewhere. But this survey, unlike the original surveys before the magnets were installed, has no constrained subsets of the data which can be independently checked to allow detection and isolation of a mistake. The weakest elements in the present survey are the lengths between monuments, which unlike the angles, were measured only once, and not with the most carefull techniques. (Although note that the three lengths measured with the tape measure are essentially perpendicular to the closure error and thus are probably not the culprits). Although a Monte Carlo analysis in Appendix B shows that, even with the relatively high random errors assumed here for the length measurements, the angle errors are the dominant contributors to all but the very low harmonics, that does not mean we are tolerant of mistakes in the length measurements. When the remainder of the magnet offset measurements are made, it should be worthwhile to repeat the intermonument length measurements, with more care for accuracy, and measuring each more than once so mistakes can be detected.

Appendix A. CLOSURE OF SURVEY DATA

A1. CLOSURE

Since three more numbers from outside the survey are needed to orient the ring - for example, the two coordinates of the first point and the bearing to the second - the redundancy in the 48 measurements is only three. Or, as another way of looking at it, the shape of the 24-gon can be determined by measuring 23 sides and the 22 angles beween them, leaving the last side and two angles as redundant measurements. Ideally, this overdetermined set of measurements will be used to give a least squares fit for the positions of the monuments. This Appendix shows such a least squares fit, done in a way which does not require the handling of large matrix equations. Also shown is a comparison with other surveyors methods of closing the traverse. These methods have the virtue of being computationally simple enough to be done with pocket calculators, or, in years past, by hand.

Starting at point 1 and applying the measured distances and angles around the N-sided monument figure brings us back to point N+1, which should be the same as point 1. The error in closure consists of dX and dY, the coordinate errors, and $d\phi$, the difference between the sum of the turning angles and 360°. The measurements are adjusted to eliminate these closure errors using what are called 'closure rules'. In all cases, the angles are first adjusted to eliminate the angle error by subtracting $d\phi/N$ from all measured angles; this is not actually necessary in the full least squares fit because the fit will take care of angle closure too. Then the dX and dY closure errors are eliminated by these rules:

1. Compass Rule(4). Each leg of the traverse consists of a dx and a dy and has a length $l^2 = dx^2 + dy^2$. The sum of all lengths is L. Each dx is adjusted by $dx' = dx - dX \cdot l/L$, and similarly for dy.

2. Transit Rule(4). Like Compass Rule, except the fractional dx correction for each leg, instead of being l/L, is |dx|/sum|dx|, and similarly for dy.

3. Crandall Rule(4). This is a least squares adjustment, but only the lengths and not the angles are adjusted, so it is valid only if the angle data are of much higher quality than the length data. This limited least squares fit is linear and leads to only two simultaneous equations, and is therefore easy to do.

4. Least Squares. (Derived below).

All these methods are relatively easy to implement on a spreadsheet, which is being used to calculate the monument and magnet positions from the survey data. All provide a geometrically correct closed figure. However, the transit rule is not rotationally invariant - its adjustments depend on the choice of the x and y directions - so it is not likely to be a good choice. Figure A1 shows the radial deviations of the monuments from their ideal positions, using the four methods of closure. Figure A2 shows the radial differences relative to that for the least squares fit. The origin in each of the four cases has been chosen independently to cancel the average x, y, and azimuth deviations from the ideal monument figure. Thus the apparent sine wave difference between the Crandall and least squares solutions, which looks like it could be due to a simple displacement of one system, is not - there are azimuth shifts causing it. The difference in radii between the various closure rules is less than

0.025 inch, which is significant, but much less than the radial deviations themselves.

A2. LEAST SQUARES FIT

Figure A3 shows a simplified traverse where N=4. The lengths l_i and turning angles ϕ_i are measured with estimated errors s_i and e_i respectively. The direction of each leg is given by

$$\theta_i = \theta_0 + \sum_{j=1}^{i} \phi_j \qquad \text{(A1)}$$

where θ_0 is an arbitrary direction, chosen (with x_1 and y_1) to orient the figure as desired.

The closure errors are

$$X \equiv x_{N+1} - x_1 \qquad \text{(A2a)}$$

$$Y \equiv y_{N+1} - y_1 \qquad \text{(A2b)}$$

$$T \equiv 2\pi - \sum_{1}^{N} \phi_i \qquad \text{(A2c)}$$

We want an adjusted set of lengths and angles, l_i' and ϕ_i', that eliminate the closure errors. Denote the length and angle residuals by d and a:

$$d_i = l_i' - l_i \qquad \text{(A3a)}$$

$$a_i = \phi_i' - \phi_i \qquad \text{(A3b)}$$

The conditions on the d's and a's to close the figure are nonlinear, but if they are small we can write a linear approximation. It is clear from Figure A3, by considering the effect of d_i or a_i on the point N+1, that closure requires

$$X = \sum_i (d_i \cos\theta_i + a_i y_i) \qquad \text{(A4a)}$$

$$Y = \sum_i (d_i \sin\theta_i - a_i x_i) \qquad \text{(A4b)}$$

$$T = \sum_i a_i \qquad \text{(A4c)}$$

The least squares solution requires minimizing the "chisquare",

$$\Psi = \sum \left(\frac{d_i}{s_i}\right)^2 + \sum \left(\frac{a_i}{e_i}\right)^2 \qquad \text{(A5)}$$

subject to the constraints A4. This can be done by using Lagrange multipliers,

minimizing a modified chisquare,

$$\psi' = \psi + A\left[X - \Sigma(d_i \cos\theta_i + a_i y_i)\right] + B\left[Y - \Sigma(d_i \sin\theta_i - a_i x_i)\right] + C\left[T - \Sigma a_i\right] \quad \text{(A6)}$$

where A, B, and C are the Lagrange multipliers. This is minimized by requiring

$$\frac{d\psi'}{dx} = 0$$

for x = d's, a's, A, B, and C. Taking the derivative with respect to the Lagrange multipliers just recovers the constraint equations A4. Taking the derivatives with respect to the residuals gives the conditions

$$\frac{d\psi'}{dd_i} = 2\,\frac{d_i}{s_i^2} - 2A\cos\theta_i - 2B\sin\theta_i = 0 \quad \text{(A7a)}$$

$$\frac{d\psi'}{da_i} = 2\,\frac{a_i}{e_i^2} - 2Ay_i + 2Bx_i - 2C = 0 \quad \text{(A7b)}$$

Solving for d and a gives

$$d_i = s_i^2\,(A\cos\theta_i + B\sin\theta_i) \quad \text{(A8a)}$$

$$a_i = e_i^2\,(Ay_i - Bx_i + C) \quad \text{(A8b)}$$

Substitute these expressions into the constraint equations A4:

$$X = \Sigma\, s_i^2\,(A\cos\theta_i + B\sin\theta_i)\cos\theta_i + \Sigma\, e_i^2\,(Ay_i - Bx_i + C)\,y_i \quad \text{(A9a)}$$

$$Y = \Sigma\, s_i^2\,(A\cos\theta_i + B\sin\theta_i)\sin\theta_i - \Sigma\, e_i^2\,(Ay_i - Bx_i + C)\,x_i \quad \text{(A9b)}$$

$$T = \Sigma\, e_i^2\,(Ay_i - Bx_i + C) \quad \text{(A9c)}$$

Regroup to get three simultaneous equations to solve for A, B, and C:

$$A[cc+yy] + B[sc-xy] + C[y] = X \qquad \text{(A10a)}$$

$$A[sc-xy] + B[ss+xx] + C[-x] = Y \qquad \text{(A10b)}$$

$$A[y] + B[-x] + C[1] = T \qquad \text{(A10c)}$$

where the coefficients in brackets [] are shorthand for the sums

$$[yy] = \sum e_i^2 y_i^2$$

$$[y] = \sum e_i^2 y_i$$

$$[sc] = \sum s_i^2 \sin\theta_i \cos\theta_i$$

$$[1] = \sum e_i^2$$

etc.

The values of A, B, and C determined from A10 are then used in A8 (and A3) to give the adjusted lengths and angles.

The covariance matrix for A, B, and C is the inverse of the 'matrix' in A10. The errors and correlations on the monument coordinates could be obtained by propagating the errors on A, B, and C through A8 and A3 to the adjusted lengths and angles, and then through the geometry equations to the coordinates. Instead, results from a Monte Carlo simulation will be presented in Appendix B.

How close is this adjusted set of values to the (unknown) true values? If the estimates of the random errors are correct, then (using x and s to mean the value and error for both lengths and angles)

$$\langle D_{m-a} \rangle = \langle \sum (x_{measured} - x_{adjusted})^2 / s^2 \rangle = 3 \qquad \text{(A11a)}$$

$$\langle D_{m-t} \rangle = \langle \sum (x_{measured} - x_{true})^2 / s^2 \rangle = 48 \qquad \text{(A11b)}$$

where the values 3 and 48 are the number of constraints and the number of variables, respectively. A measure of correctness of the adjusted values is

$$D_{a-t} = \sum (x_{adjusted} - x_{true})^2 / s^2 \qquad \text{(A12)}$$

A little algebra shows that

$$D_{a-t} = D_{m-t} - D_{m-a} + \sum (x_{meas} - x_{adj})(x_{adj} - x_{true})/s^2 \qquad \text{(A13)}$$

As earlier, use d and a for length and angle differences (adjusted - measured), and use d' and a' for the differences (adjusted - true). Then, using equation A8 for d and a, the last term may be rewritten

$$\begin{aligned} &\sum d_i d_i'/s_i^2 + \sum a_i a_i'/e_i^2 \\ &= \sum (A\cos\theta_i + B\sin\theta_i) d_i' + \sum (Ay_i - Bx_i + C) a_i' \\ &= A \sum (d_i' \cos\theta_i + a_i' y_i) \\ &+ B \sum (d_i' \sin\theta_i - a_i' x_i) \\ &+ C \sum a_i' \end{aligned} \qquad \text{(A14)}$$

Since both the adjusted and the true values satisfy the constraints, the A, B, and C terms vanish, by equation A4, and thus

$$D_{a-t} = D_{m-t} - D_{m-a} \qquad \text{(A15)}$$

Note that A15 is true not only for expected values, but for actual values in each individual case.

Appendix B. MONTE CARLO OF SURVEY TECHNIQUE

B1. MONTE CARLO

Simulated sets of survey data were created by adding random gaussian (normal) deviates to the lengths and angles of the ideal monument figure (1348.44 in. and 15 degrees). The gaussians were generated from the formula

$$g_i = \sqrt{-2 \ln r_i} \cdot \cos(2\pi r_{i+1}) \qquad \text{(B1a)}$$

$$g_{i+1} = \sqrt{-2 \ln r_i} \cdot \sin(2\pi r_{i+1}) \qquad \text{(B1b)}$$

where r is a random number with a uniform distribution from 0 to 1, and g is a random number with a gaussian distribution with mean=0 and sigma=1. (This formula is in common use but its derivation is not obvious; perhaps a note should be published showing why it works). Note that two independent gaussians are generated from each pair of uniform random numbers.

This simulated data was then 'closed' by the same methods as the real data. The least squares fit on the average gave the answer closest to the true values, although occassionally one of the other methods was better. Figures B1 - B3 show the distributions of the weighted sum of squares for each of the three differences between the true, measured, and adjusted values. These should be chi-square distributions with 3 (for measured-adjusted), 48 (measured-true), and 45 (adjusted-true) degrees of freedom.

All Monte Carlo results here use the ideal monument figure (i.e., equal sides and 15 degree angles) as the starting point.

B2. FOURIER ANALYSIS

Since the magnets are surveyed relative to the monuments, the errors in the monuments will propagate to the magnets and thus affect the beam. Thus it is interesting to see the harmonic content of the survey errors. For each of the 250 Monte Carlo runs, the radial deviations were Fourier analysed, with the average amplitudes of the components shown in Figure B4. The first harmonic corresponds only to a uniform shift of all monuments and will have no effect on the machine; it is nonzero here because the center was not redefined for each of the Monte Carlo runs. The distribution of amplitudes for the 9th harmonic is shown in Figure B5.

Separate Monte Carlos were run with only length errors, or only angle errors, with the results included in the Figure B4. With the sigmas used here, the length and angle error have comparable contributions to the lowest harmonics, but the relative effect of the length errors decreases at higher harmonics. For the 9th harmonic the average amplitudes are

sig-len	sig-ang	<amp.-9th>
0.014 in	0.6 sec	0.000498 in
0.014	none	0.000218
none	0.6	0.000463

Note that these results were obtained using estimated length and angle errors which gave, on the actual survey, a large chi-square. If the large chi-square is due to an underestimate of the errors (and not a mistake), then the estimated errors should be increased by a factor of 9.4/3 = 1.8, and the Monte Carlo estimates will all increase by the same factor.

B3. ERRORS IN COORDINATES

The position of each monument is determined by the survey to within some error ellipse. By symmetry (ignoring the complication due to the use of the temporary monument in the real world), the error ellipses should have their axes along the radial and azimuthal directions, and should be the same for each monument. Of more interest are the errors of one monument relative to another, taking correlations into account. These can be determined from the Monte Carlo data, but there are many possible ways to do it, depending on just which correlations are chosen to be removed and which ones to stay. We want to see the effect of "bumpiness" in the monument figure, but not the effect of things like translations or rotations of the whole figure, which do not affect the physics of the AGS. The results here are from one choice, which is a compromise between trying to understand what is physically significant, and what was computationally feasible.

Figures B6 - B8 show the radial and azimuthal errors of each point, relative to monument LA. For each of the three figures, 250 data sets were generated with both length and angle errors, length errors only, or angle errors only. Each of the data sets was closed, translated, and rotated, as described for the actual survey data, to give a set of monument coordinates. What is plotted is the rms errors, relative to the first monument, projected into the radial and azimuthal directions:

$$dx_i = (x_i - x_i^\circ) - (x_1 - x_1^\circ) \qquad \text{(B2a)}$$

$$dy_i = (y_i - y_i^\circ) - (y_1 - y_1^\circ) \qquad \text{(B2b)}$$

$$dr_i = dx_i \cos\theta_i + dy_i \sin\theta_i \qquad \text{(B3a)}$$

$$da_i = dy_i \cos\theta_i - dx_i \sin\theta_i \qquad \text{(B3b)}$$

$$dr_i(\text{rms}) = \sqrt{\sum dr_i^2 / N} \qquad \text{(B4a)}$$

$$da_i(\text{rms}) = \sqrt{\sum da_i^2 / N} \qquad \text{(B4b)}$$

where (x_i°, y_i°) is the ideal location of monument i, and θ_i is the azimuthal position of monument i (multiples of 15 degrees).

The error ellipses for these relative errors do not necessarily have their axes along the radial and azimuthal directions. The correlations which give the axis directions could be calculated from the Monte Carlo data if needed, but it is not done here.

The effect of the variation in average radius has not been removed from the figures, although perhaps it should be, because a change in average radius will not cause orbit distortions. The amount of average radius change, dR, is shown below. Also shown, in the last two columns, are the rms radial and azimuthal errors, relative to the center of the figure (not relative to

monument LA).

sig-len	sig-ang	dR (rms)	dr (rms)	da (rms)
0.014 in	0.6 sec	0.0115	0.0154	0.0158
0.014	none	0.0115	0.0134	0.0150
none	0.6	0	0.0074	0.0049

B4. EFFECT OF SINGLE MEASUREMENT ERRORS

It is not intuitively obvious how a single measuring error - either a statistical error or a blunder - propagates through the closure calculations and affects the monuments. Figures B9 and B10 show the monument displacements caused by a single length error (.014 inch) or angle error (0.6 sec), respectively. Figure B11 shows the fourier components caused by this distortion. Figure B12 shows the deviations of the real monuments from their ideal locations (with a very different magnification) in case anyone would like to guess where there might be blunders in the survey data.

REFERENCES

1. O. S. Reading, "Interim Data on the Stability of AGS Foundations", BNL Accelerator Development Department Internal Report OSR-4, January 26, 1960, and "Alignment Stability of the 33-BeV Synchrotron at Brookhaven National Laboratory, 1959-1962", BNL Accelerator Department Internal Report OSR-5, July 15, 1964.

2. H. S. Snyder. "The Monument Survey" BNL Accelerator Development Department Internal Report HSS-3, October 7, 1954.

3. L. J. Laslett and L. Smith. "Analysis of Surveying Procedures That Only Employ Distance Measurements and the Effect of Surveying Errors on the Closed Orbit", LBL-UCID-10161.

4. R. E. Davis and F. S. Foote, Surveying Theory and Practice, McGraw-Hill, 1953.

FIGURE CAPTIONS

1. Radial deviations, present survey and 1962 survey.

2. Present radial deviations, compared with 1962 deviations multiplied by 4.

3. X and y deviations of present survey and old surveys. The present points are plotted using dx and dy, and because of the size of the deviations, and the curvature of the polar coordinate system, do not accurately represent dr and da. See Figure B12 for another picture.

A1. Radial deviations for various closure methods, relative to ideal positions.

A2. Radial deviations for various closure methods, relative to least squares fit.

A3. Simple traverse, showing geometry for least squares fit.

B1. Distribution of weighted sum-of-squares of "measured" minus "adjusted" values (i.e., "chi-square") for 250 Monte Carlo runs. These plots use bar charts to simulate histograms; the number ticks should be interpreted as the left edge of the bin.

B2. Distribution of weighted sum-of-squares of "measured" minus "true" values.

B3. Distribution of weighted sum-of-squares of "adjusted" minus "true" values.

B4. Fourier amplitudes of Monte Carlo data. (The 12th harmonic should be half that shown).

B5. Distribution of amplitudes of 9th harmonic.

B6. Radial and azimuthal errors (rms) relative to monument LA, from Monte Carlo data with length and angle errors.

B7. Radial and azimuthal errors (rms) relative to monument LA, from Monte Carlo data with length errors only.

B8. Radial and azimuthal errors (rms) relative to monument LA, from Monte Carlo data with angle errors only.

B9. Monument displacements for a single .014 inch length measurement error.

B10. Monument displacements for a single 0.6 second angle measurement error.

B11. Harmonics generated by the displacements of Figures B9 and B10.

B12. Displacements of "actual" monuments from ideal locations. Note that the scale of the displacements is much different from Figures B9 and B10.

TABLE 1. Monument survey data with least-squares fit for coordinates.
The data and coordinates in this table use 'temporary' monument fg'.

Monument		Measured deg	min	sec	angle	length	Adjusted angle	length	Residuals angle(sec)	length	Coordinates X	Y
1	la	15	0	8.7	15.002417	1348.408	15.002470	1348.407	0.193	-0.0004	-4989.331	1336.864
2	a	14	59	49.6	14.997111	1348.370	14.997138	1348.371	0.100	0.0017	-5165.298	-0.012
3	ab	15	0	5.3	15.001472	1348.401	15.001474	1348.404	0.009	0.0036	-4989.331	-1336.853
4	b	15	0	3.9	15.001083	1348.423	15.001062	1348.427	-0.074	0.0052	-4473.316	-2582.615
5	bc	14	59	59.6	14.999889	1348.424	14.999848	1348.430	-0.144	0.0066	-3652.423	-3652.378
6	c	14	59	56.3	14.998972	1348.378	14.998918	1348.385	-0.194	0.0074	-2582.625	-4473.230
7	cd	14	59	49.6	14.997111	1348.401	14.997049	1348.408	-0.223	0.0078	-1336.880	-4989.236
8	d	15	0	10.5	15.002917	1348.399	15.002853	1348.406	-0.227	0.0076	-0.016	-5165.308
9	de	14	59	53.7	14.998250	1348.345	14.998192	1348.352	-0.207	0.0069	1336.855	-4989.308
10	e	15	0	19.3	15.005361	1348.458	15.005315	1348.463	-0.164	0.0058	2582.587	-4473.358
11	ef	14	59	41.4	14.994833	1348.452	14.994805	1348.455	-0.101	0.0042	3652.347	-3652.402
12	f	12	11	14.3	12.187306	1036.920	12.187299	1036.930	-0.022	0.0109	4473.269	-2582.626
13	fg'	16	42	57.7	16.716028	1664.079	16.716040	1664.081	0.045	0.0021	4916.647	-1645.267
14	g	16	5	56.8	16.099111	1348.392	16.099155	1348.390	0.160	-0.0017	5165.442	0.110
15	gh	15	0	39.2	15.010889	1348.317	15.010958	1348.302	0.252	-0.0143	4989.426	1336.963
16	h	14	58	54.4	14.981778	1348.444	14.981870	1348.438	0.335	-0.0052	4473.199	2582.528
17	hi	15	0	21.9	15.006083	1348.438	15.006195	1348.431	0.404	-0.0066	3652.443	3652.409
18	i	15	0	4.0	15.001111	1348.406	15.001237	1348.398	0.454	-0.0074	2582.664	4473.287
19	ij	15	0	4.5	15.001250	1348.422	15.001384	1348.414	0.483	-0.0078	1336.898	4989.276
20	j	14	59	46.1	14.996139	1348.383	14.996274	1348.375	0.487	-0.0076	0.012	5165.225
21	jk	15	0	13.6	15.003778	1348.450	15.003907	1348.442	0.467	-0.0069	-1336.831	4989.259
22	k	14	59	42.6	14.995167	1348.457	14.995284	1348.450	0.424	-0.0058	-2582.607	4473.178
23	kl	15	0	2.9	15.000806	1348.382	15.000905	1348.377	0.361	-0.0042	-3652.437	3652.334
24	l	15	0	1.0	15.000278	1348.400	15.000356	1348.397	0.283	-0.0024	-4473.302	2582.613
(1)	(la)										-4989.331	1336.864

		Raw	Fitted		Sum of squares:	
Closure errors:	Angle:	-3.1	0.0E+00	seconds	1.9E+00	1.0E-03
	X:	-0.209	-1.1E-07	inches	Weighted:	
	Y:	0.017	-1.4E-06	inches	5.400827	4.039403
					Total Chisquare:	
					9.440231	

Data to locate permanent monument fg:
Distance from fg to g: 1348.392
Angle fg-g-gh: 15.008611
(turning angle)

TABLE 2. Monument coordinates (X-Y and polar) and deviations from ideal coordinates. This table uses permanent monument fg.

Monument	Coordinates X	Coordinates Y	Polar Coord. radius	Polar Coord. azimuth	Deviations (x-y) dx	Deviations (x-y) dy	Dev. (polar) dr	Dev. (polar) da
1 la	-4989.331	1336.864	5165.330	165.000246	0.062	-0.040	-0.070	0.022
2 a	-5165.298	-0.012	5165.298	-179.999863	0.102	-0.012	-0.102	0.012
3 ab	-4989.331	-1336.853	5165.327	-165.000370	0.062	0.051	-0.073	-0.033
4 b	-4473.316	-2582.615	5165.313	-150.000531	0.052	0.085	-0.087	-0.048
5 bc	-3652.423	-3652.378	5165.274	-135.000354	0.067	0.112	-0.126	-0.032
6 c	-2582.625	-4473.230	5165.244	-120.000045	0.075	0.137	-0.156	-0.004
7 cd	-1336.880	-4989.236	5165.242	-105.000200	0.024	0.158	-0.158	-0.018
8 d	-0.016	-5165.308	5165.308	-90.000181	-0.016	0.092	-0.092	-0.016
9 de	1336.855	-4989.308	5165.305	-75.000279	-0.049	0.085	-0.095	-0.025
10 e	2582.587	-4473.358	5165.335	-60.001029	-0.113	0.010	-0.065	-0.093
11 ef	3652.347	-3652.402	5165.238	-45.000429	-0.142	0.087	-0.162	-0.039
12 f	4473.269	-2582.626	5165.277	-29.999836	-0.099	0.074	-0.123	0.015
13 fg	4989.257	-1336.722	5165.221	-14.998439	-0.137	0.182	-0.179	0.141
14 g	5165.442	0.110	5165.442	0.001225	0.042	0.110	0.042	0.110
15 gh	4989.426	1336.963	5165.447	15.000542	0.032	0.059	0.047	0.049
16 h	4473.199	2582.528	5165.168	29.999277	-0.168	-0.172	-0.232	-0.065
17 hi	3652.443	3652.409	5165.310	44.999729	-0.046	-0.081	-0.090	-0.024
18 i	2582.664	4473.287	5165.312	59.999895	-0.036	-0.081	-0.088	-0.009
19 ij	1336.898	4989.276	5165.285	74.999727	-0.006	-0.117	-0.115	-0.025
20 j	0.012	5165.225	5165.225	89.999863	0.012	-0.175	-0.175	-0.012
21 jk	-1336.831	4989.259	5165.252	104.999608	0.072	-0.134	-0.148	-0.035
22 k	-2582.607	4473.178	5165.190	120.000163	0.093	-0.190	-0.210	0.015
23 kl	-3652.437	3652.334	5165.253	135.000807	0.052	-0.155	-0.147	0.073
24 l	-4473.302	2582.613	5165.299	150.000474	0.066	-0.087	-0.101	0.043
(1) (la)	-4989.331	1336.864	5165.330	165.000246				
averages	0.000	-0.000	5165.287		0.000	-0.000	-0.113	0.000

Figure 1

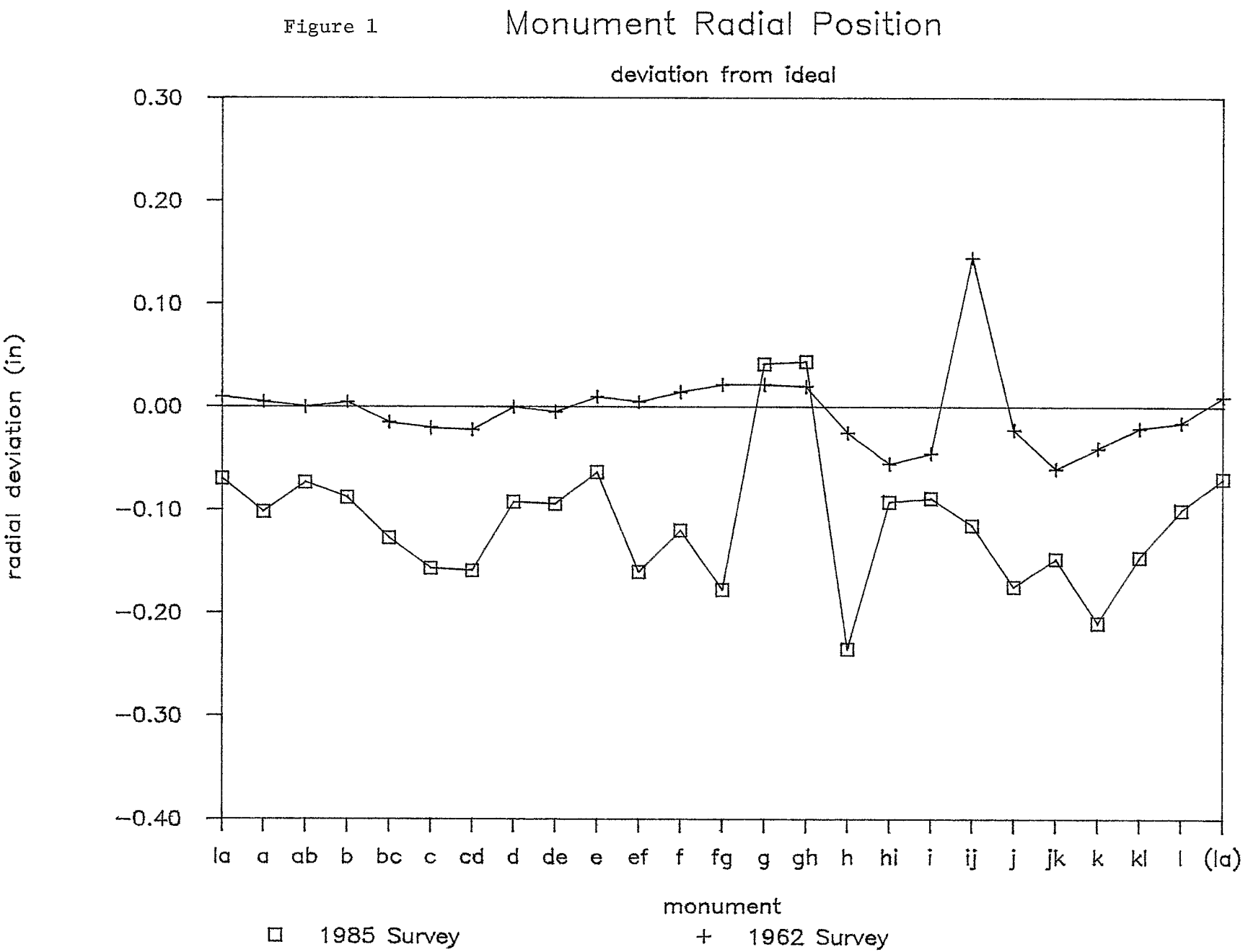
Monument Radial Position
deviation from ideal
radial deviation (in)
0.30
0.20
0.10
0.00
−0.10
−0.20
−0.30
−0.40
la a ab b bc c cd d de e ef f fg g gh h hi i ij j jk k kl l (la)
monument
1985 Survey
1962 Survey

Figure 2

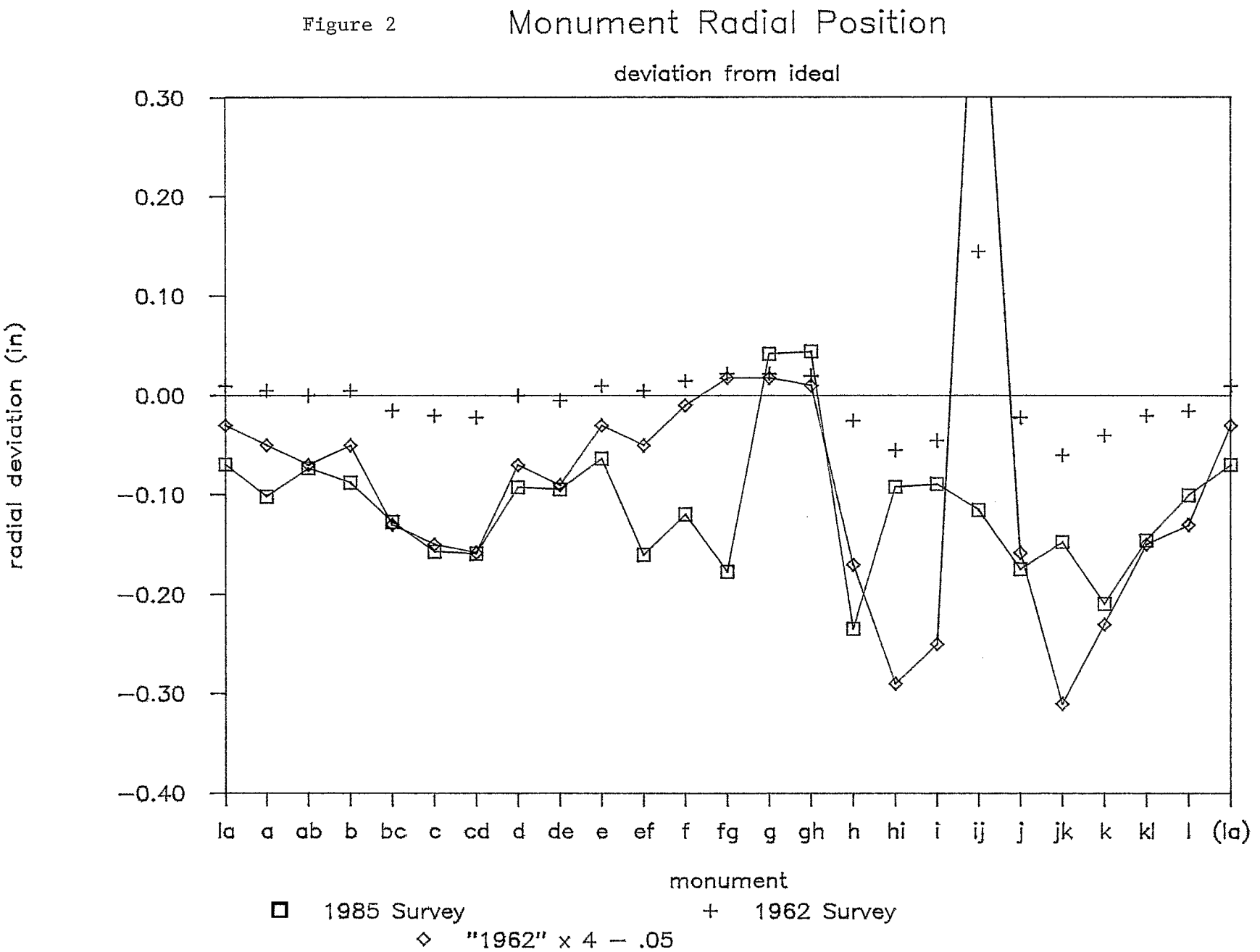
Monument Radial Position
deviation from ideal
radial deviation (in)
0.30
0.20
0.10
0.00
−0.10
−0.20
−0.30
−0.40
la a ab b bc c cd d de e ef f fg g gh h hi i ij j jk k kl l (la)
monument
1985 Survey
1962 Survey
"1962" x 4 − .05

AGS SURVEY

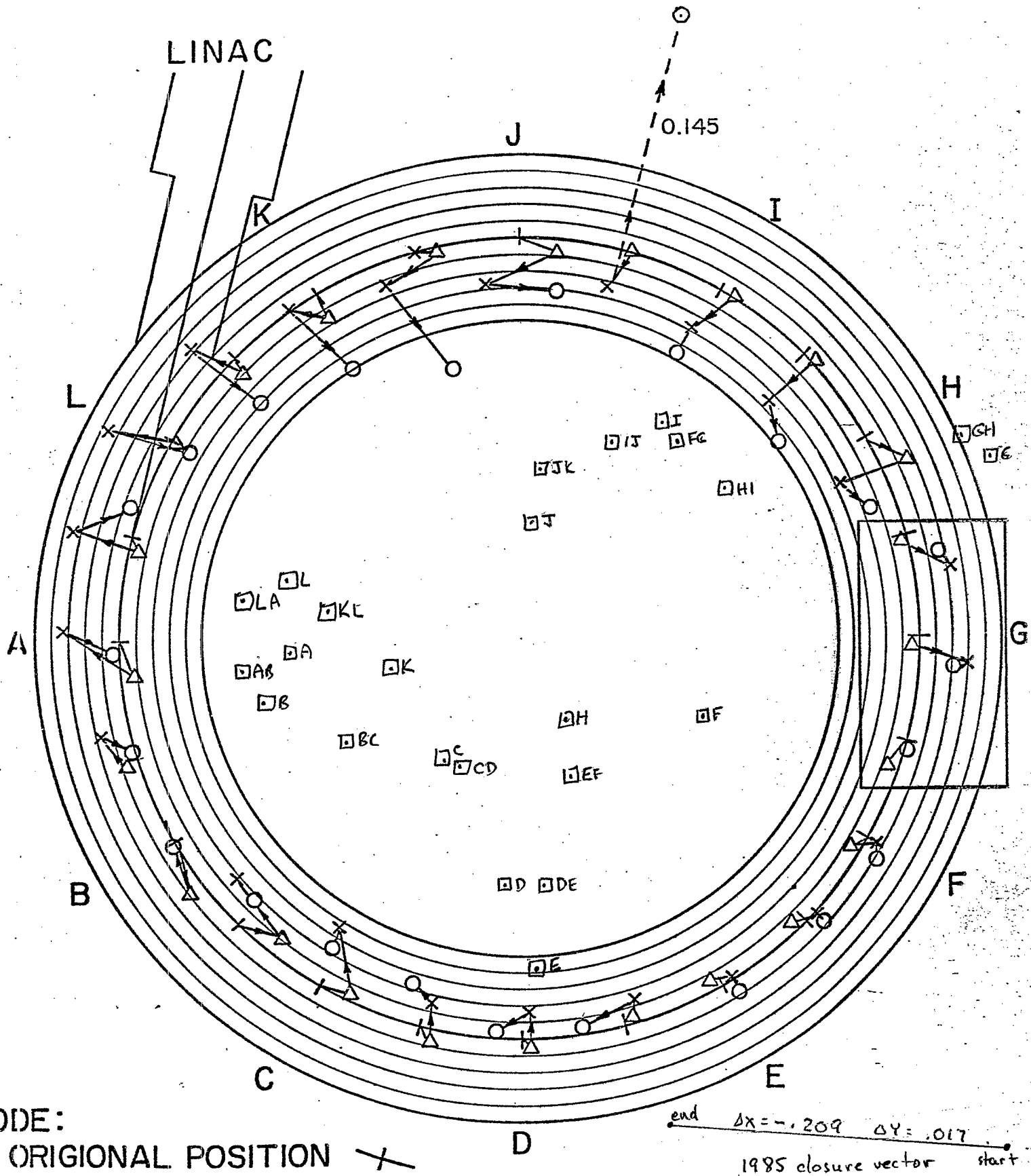

CODE:

ORIGIONAL POSITION ×

DEC. 1959 △ 1985 ⊡

OCT. 1961 ×

SEPT. 1962 ○

SCALE

Figure A1

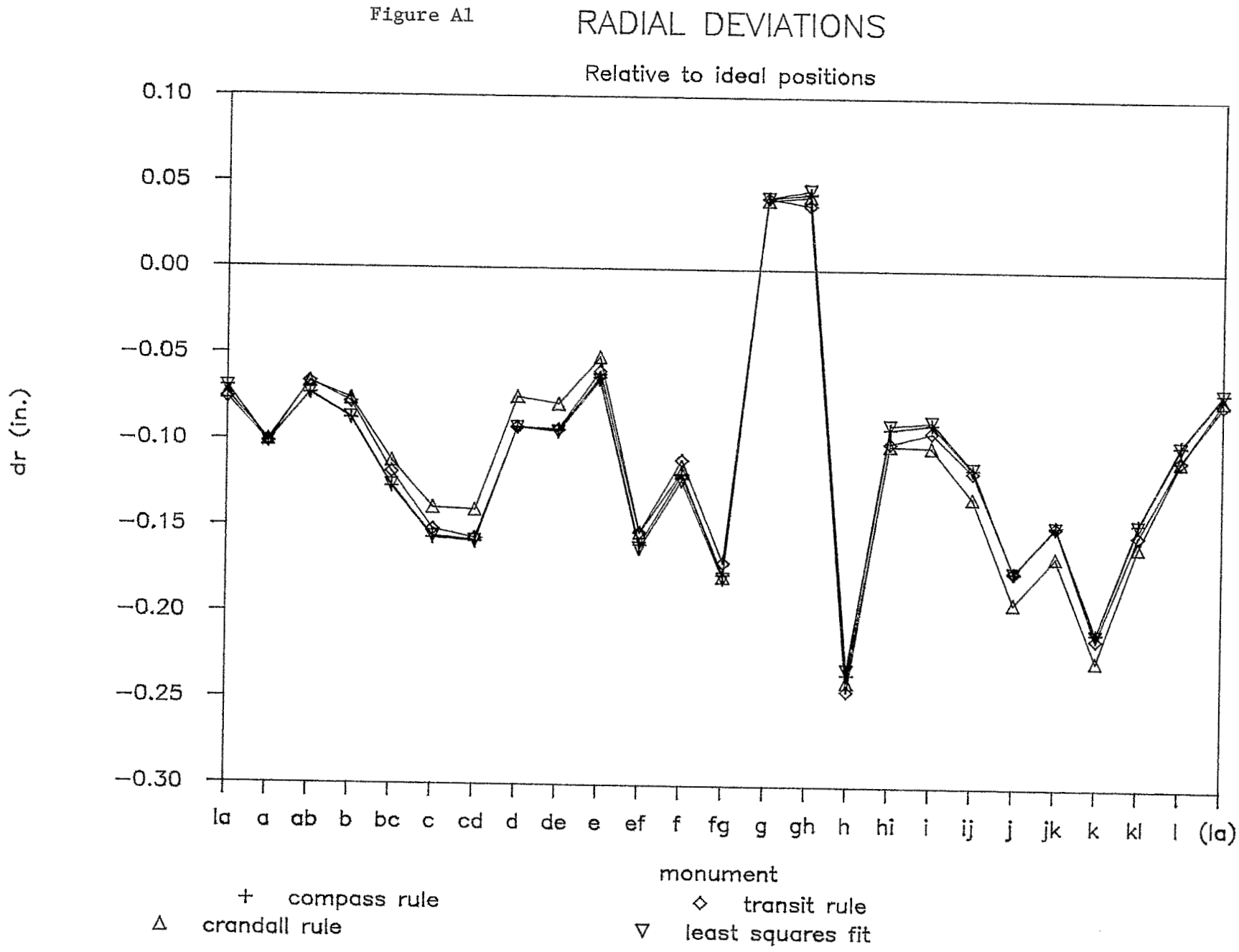
RADIAL DEVIATIONS
Relative to ideal positions
0.10
0.05
0.00
−0.05
−0.10
−0.15
−0.20
−0.25
−0.30
dr (in.)
la a ab b bc c cd d de e ef f fg g gh h hi i ij j jk k kl l (la)
monument
+ compass rule
△ crandall rule
◇ transit rule
▽ least squares fit

Figure A2

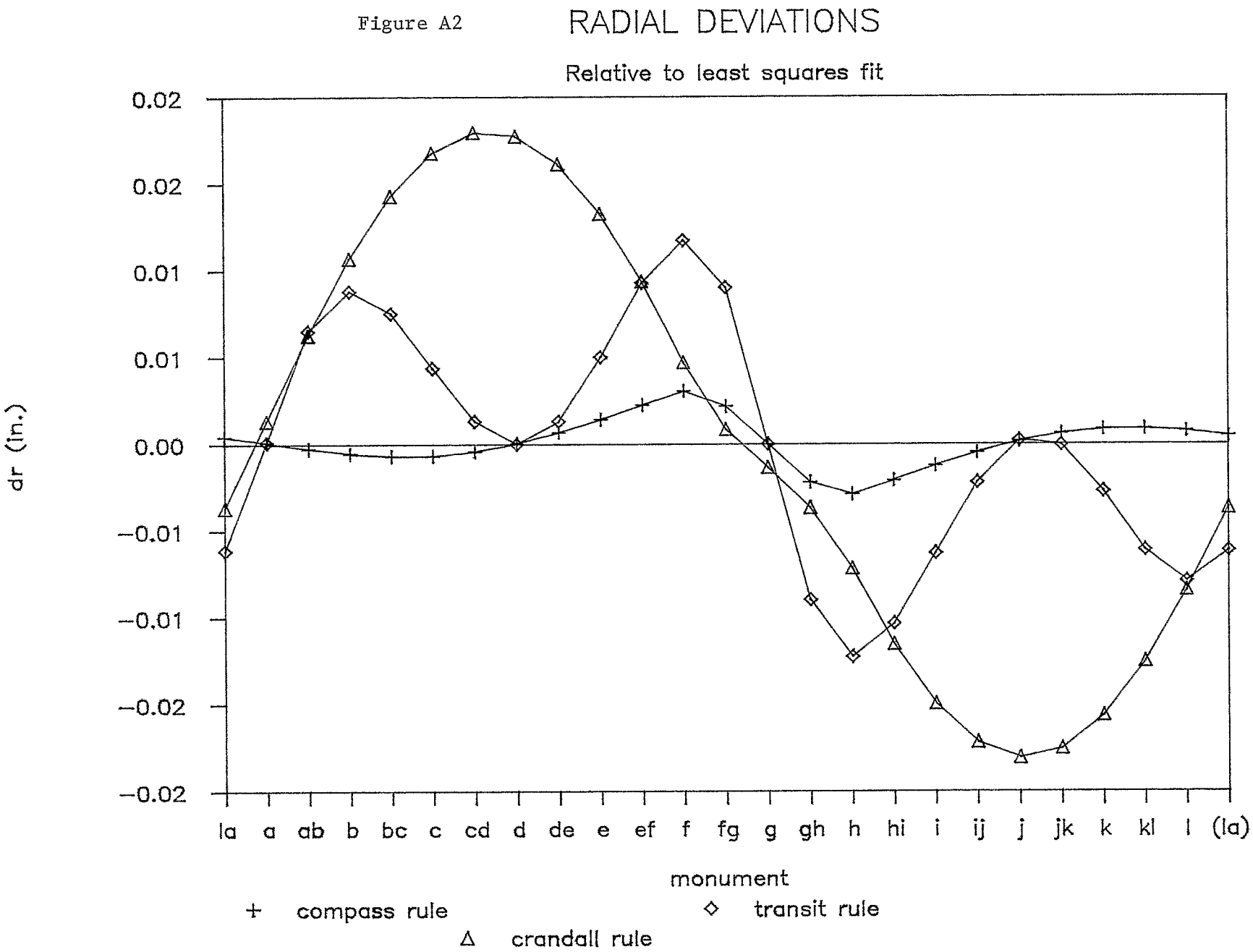
RADIAL DEVIATIONS
Relative to least squares fit
0.02
0.02
0.01
0.01
0.00
−0.01
−0.01
−0.02
−0.02
dr (in.)
la a ab b bc c cd d de e ef f fg g gh h hi i ij j jk k kl l (la)
monument
+ compass rule
◇ transit rule
△ crandall rule

Figure A3 .

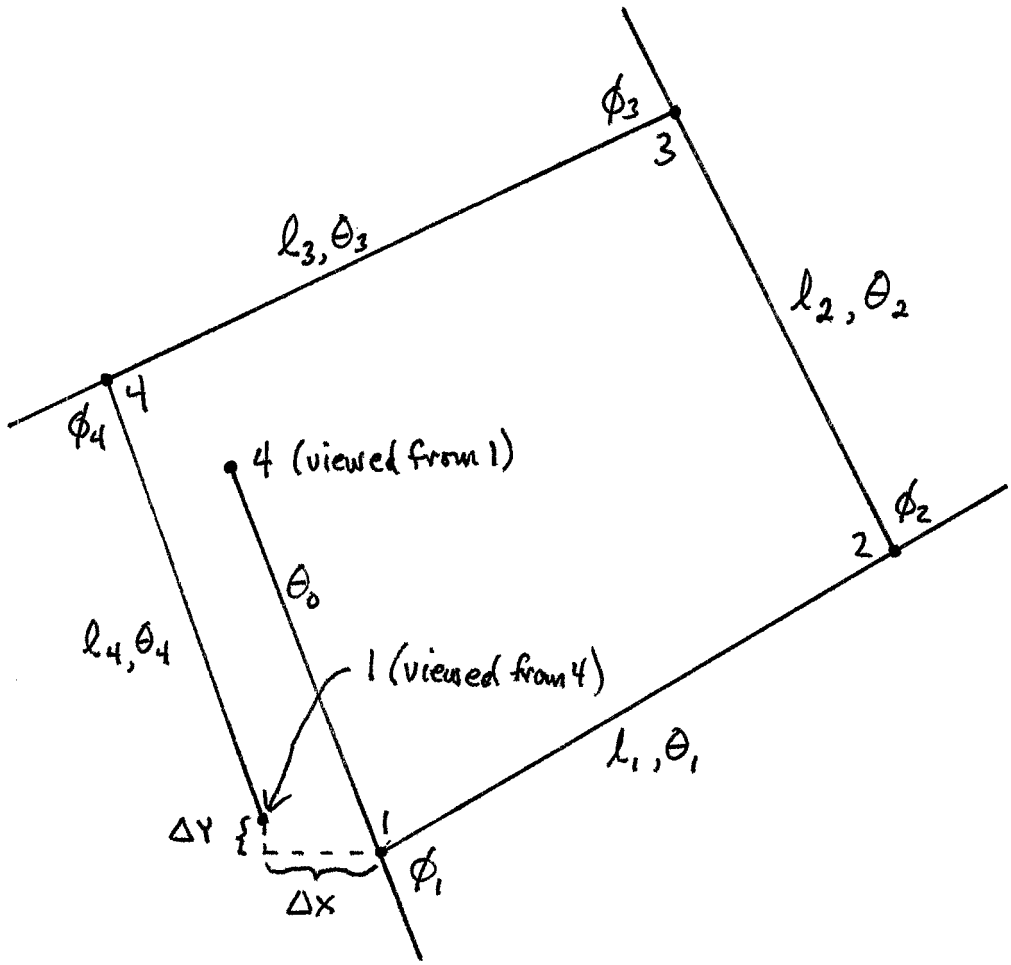
ϕ_3
3
ℓ_3, θ_3
ℓ_2, θ_2
4
ϕ_4
4 (viewed from 1)
ϕ_2
2
θ_0
ℓ_4, θ_4
1 (viewed from 4)
ℓ_1, θ_1
ΔY
1
ϕ_1
ΔX

Figure B1

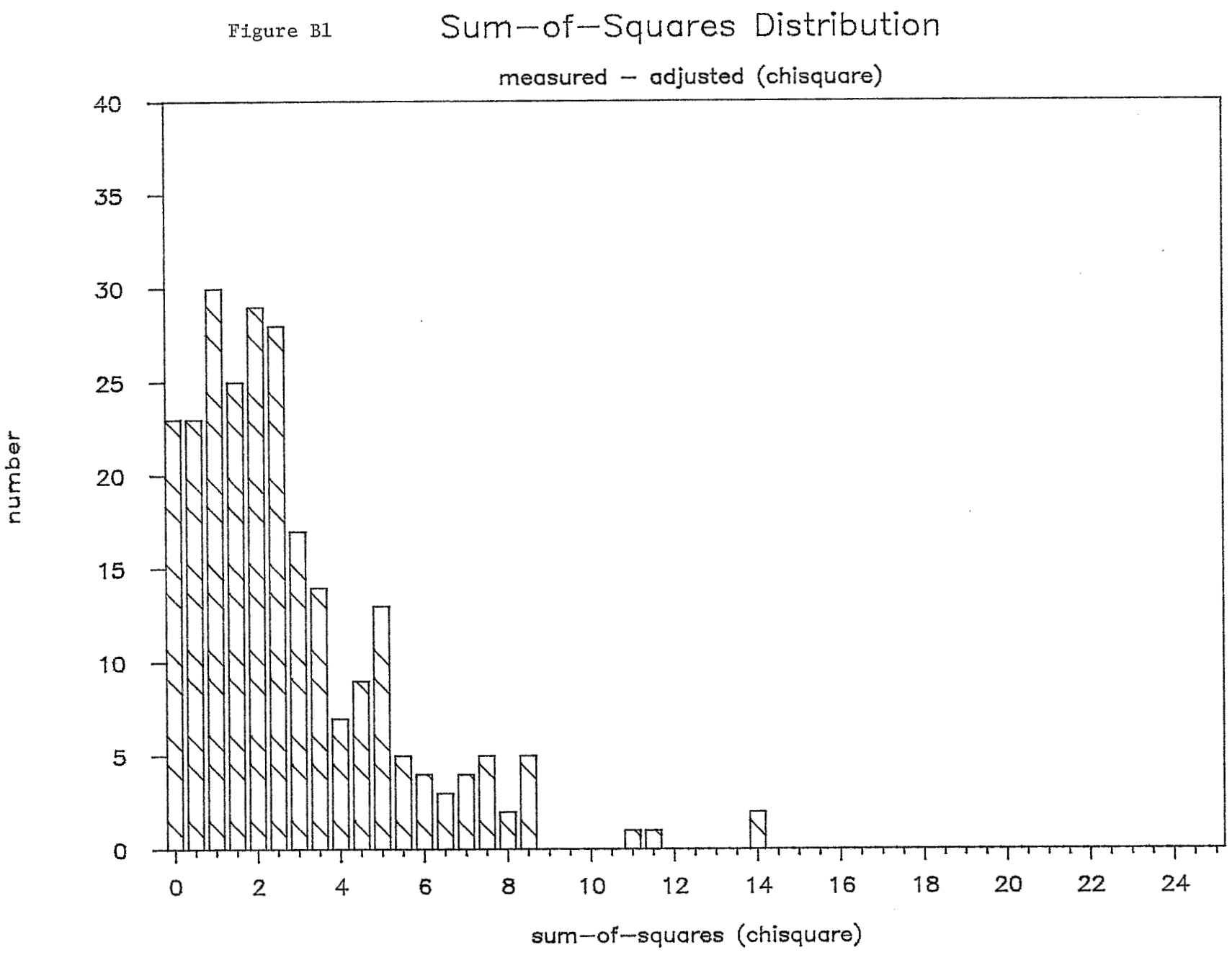
Sum—of—Squares Distribution
measured — adjusted (chisquare)
number
sum—of—squares (chisquare)
0
5
10
15
20
25
30
35
40
0
2
4
6
8
10
12
14
16
18
20
22
24

Figure B2

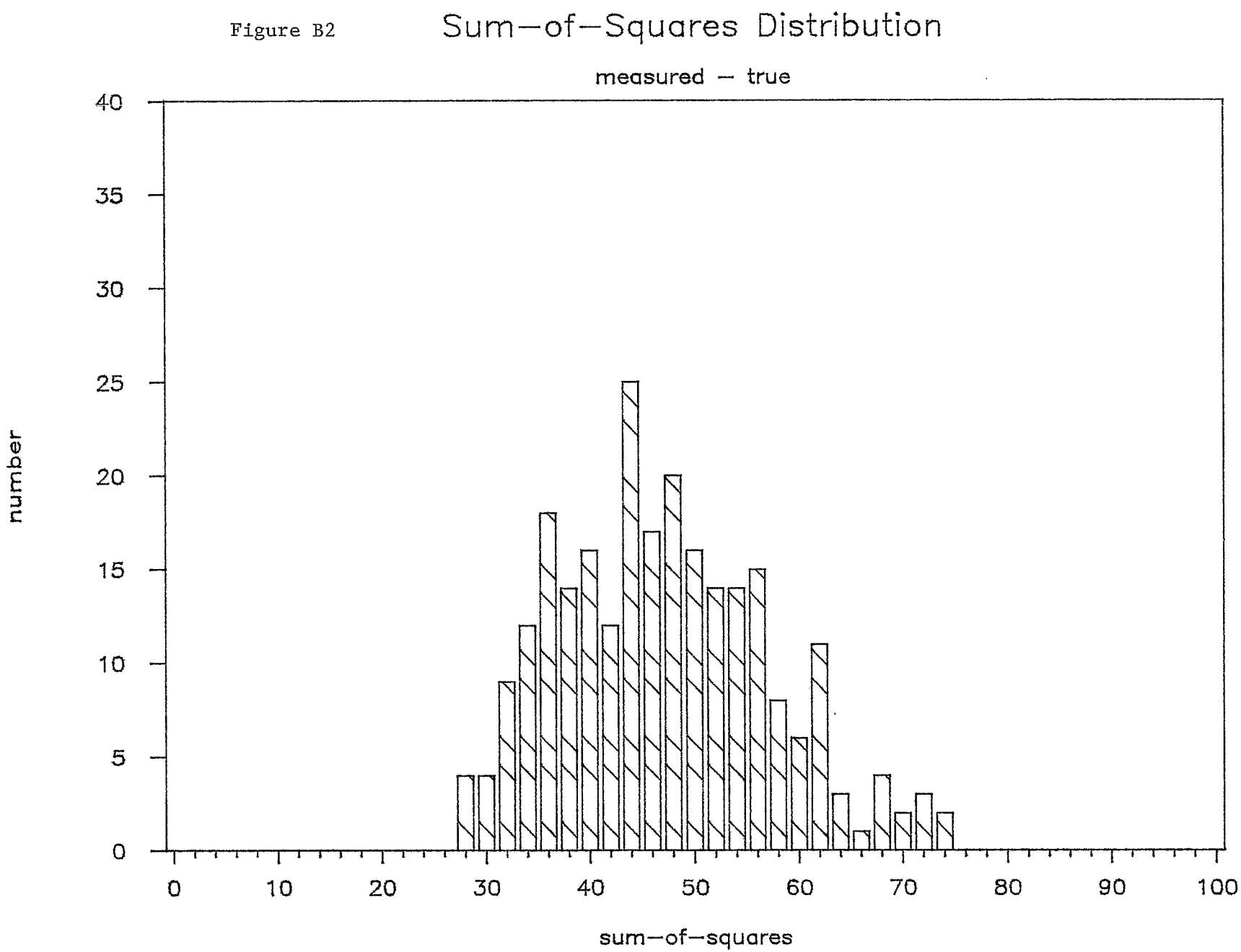
Sum—of—Squares Distribution
measured — true
number
sum—of—squares
0
5
10
15
20
25
30
35
40
0
10
20
30
40
50
60
70
80
90
100

Figure B3

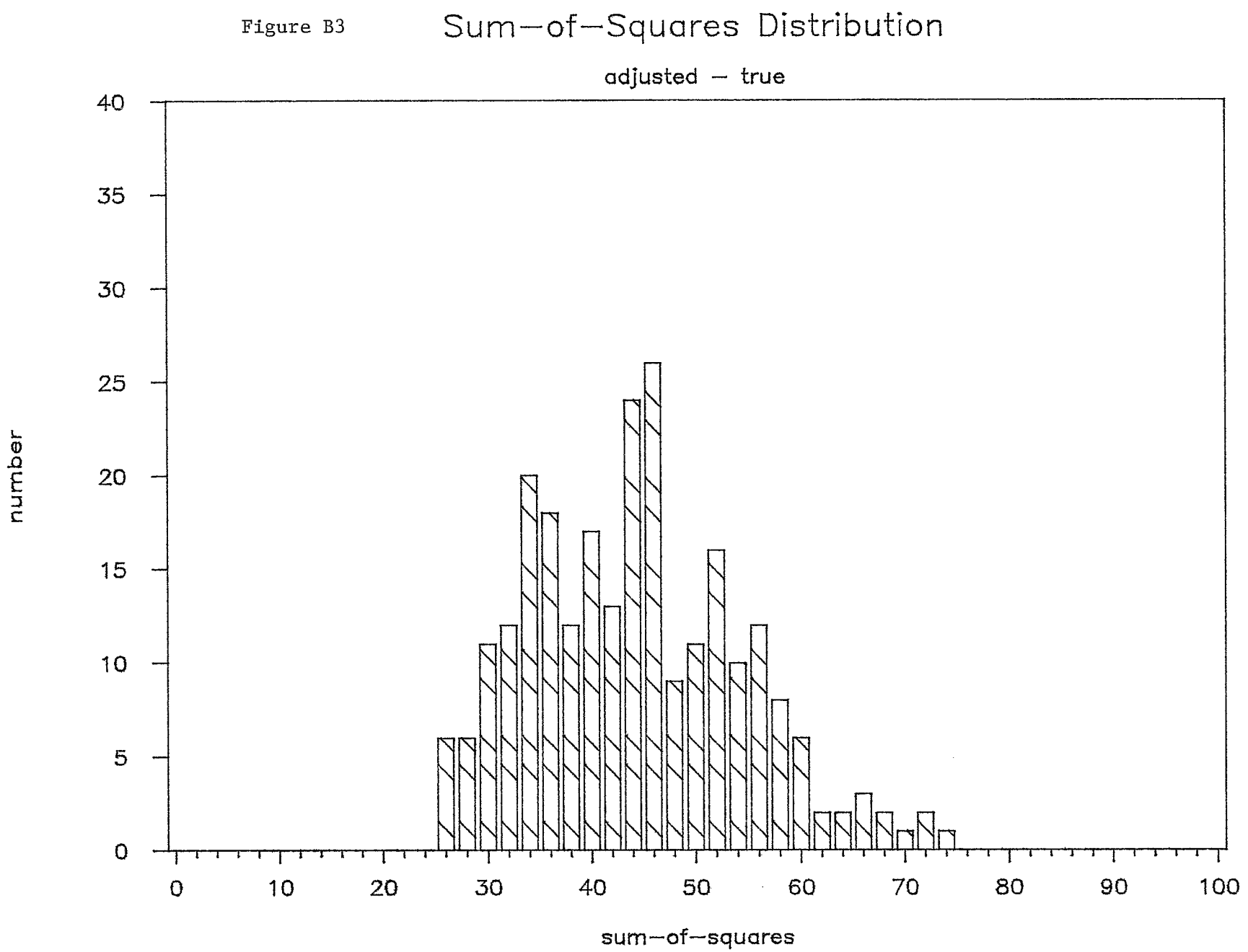
Sum—of—Squares Distribution
adjusted — true
number
sum—of—squares
0
5
10
15
20
25
30
35
40
0
10
20
30
40
50
60
70
80
90
100

Figure B4

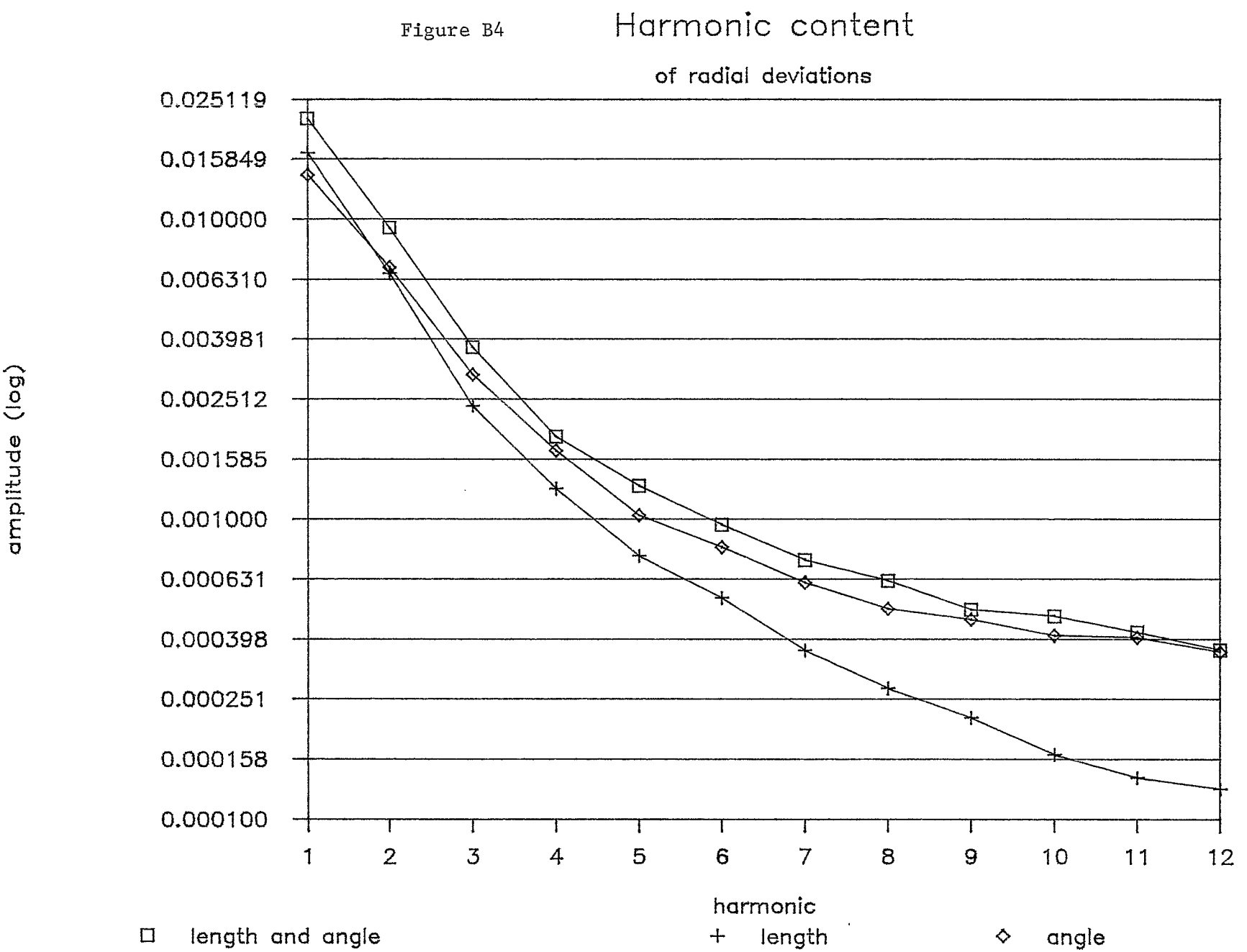
Harmonic content
of radial deviations
amplitude (log)
0.025119
0.015849
0.010000
0.006310
0.003981
0.002512
0.001585
0.001000
0.000631
0.000398
0.000251
0.000158
0.000100
1
2
3
4
5
6
7
8
9
10
11
12
harmonic
length and angle
length
angle

Figure B5

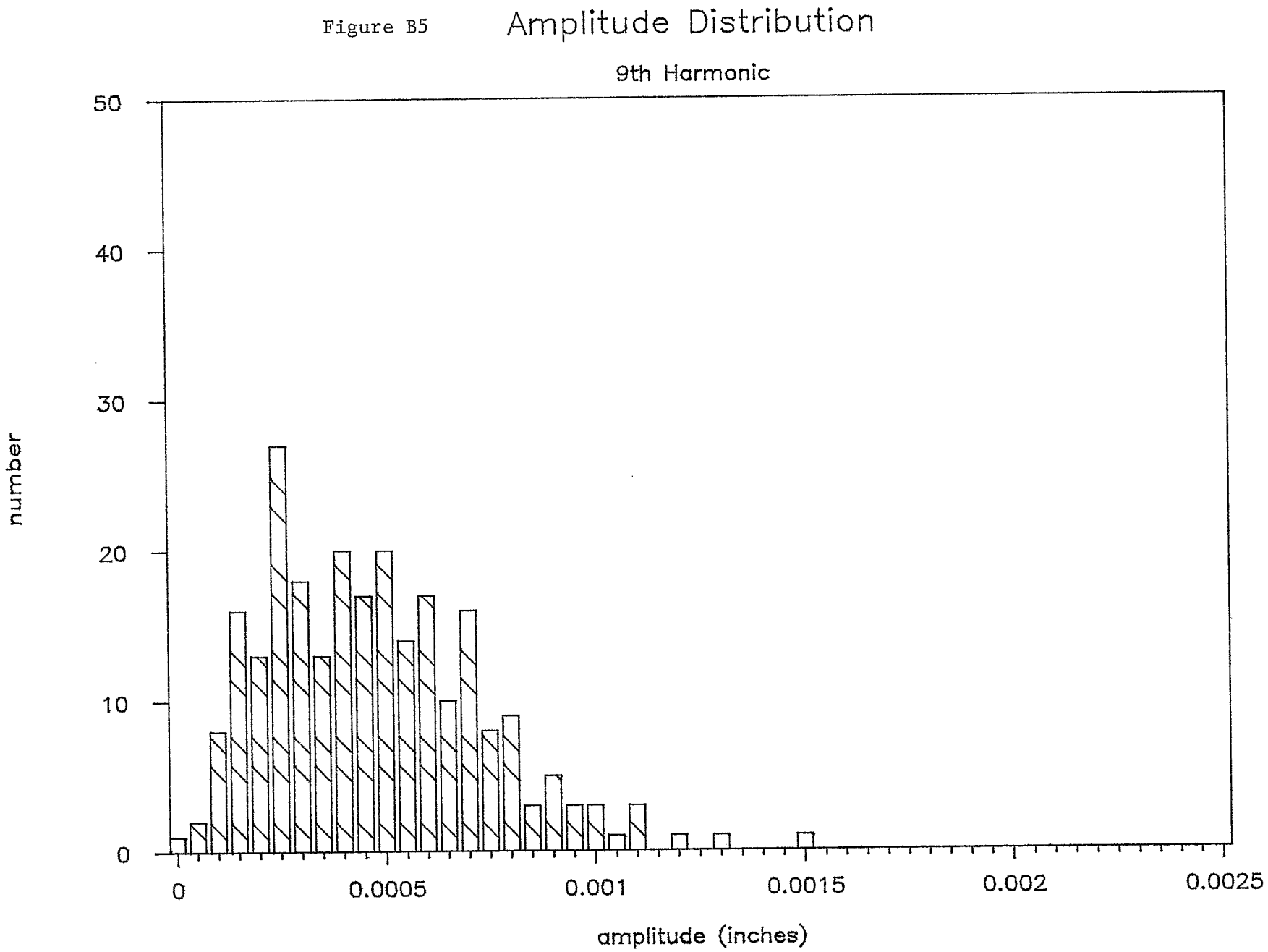
Amplitude Distribution
9th Harmonic
50
40
30
20
10
0
number
0
0.0005
0.001
0.0015
0.002
0.0025
amplitude (inches)

Figure B6

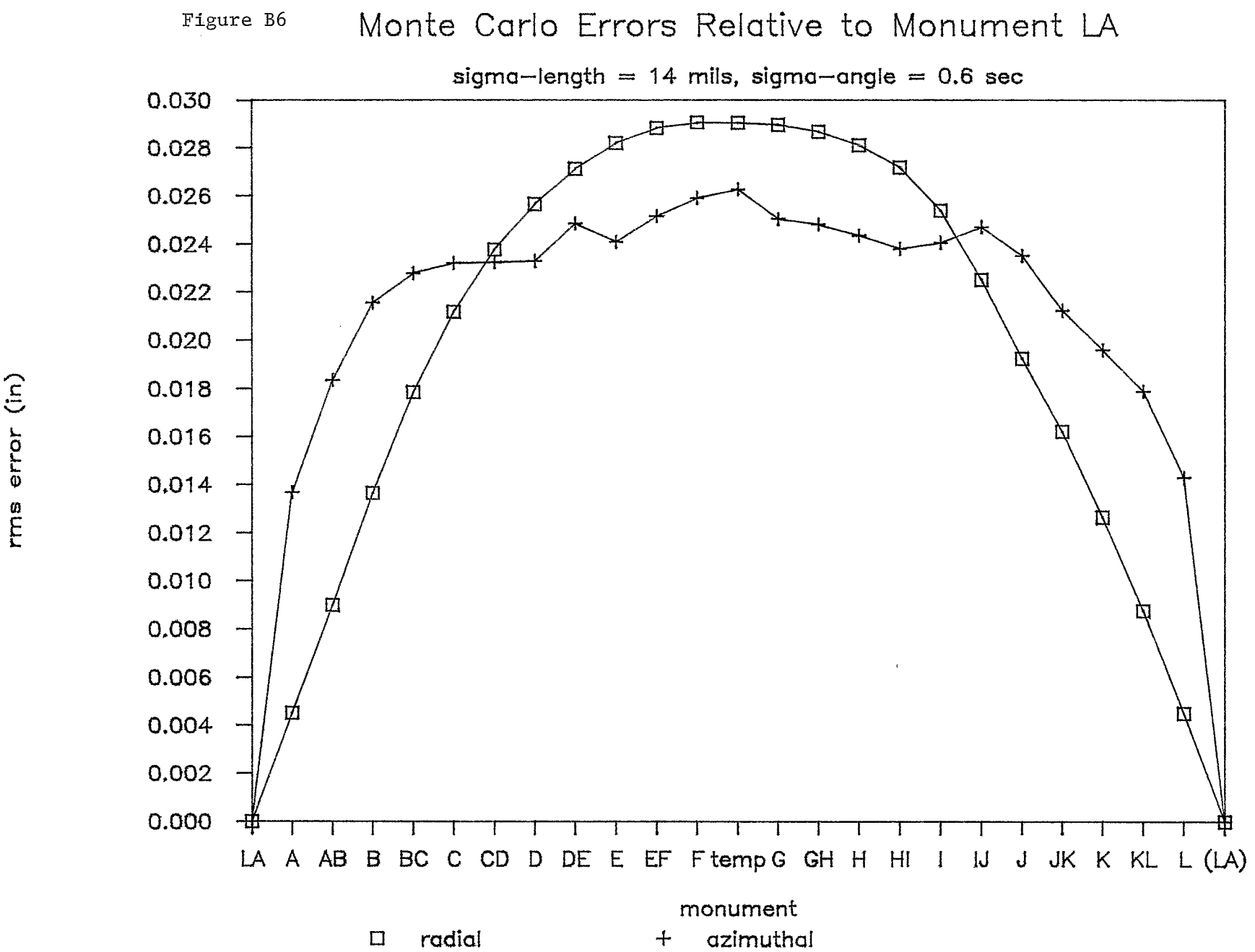
Monte Carlo Errors Relative to Monument LA
sigma–length = 14 mils, sigma–angle = 0.6 sec
rms error (in)
0.030
0.028
0.026
0.024
0.022
0.020
0.018
0.016
0.014
0.012
0.010
0.008
0.006
0.004
0.002
0.000
LA A AB B BC C CD D DE E EF F temp G GH H HI I IJ J JK K KL L (LA)
monument
radial
azimuthal

Figure B7

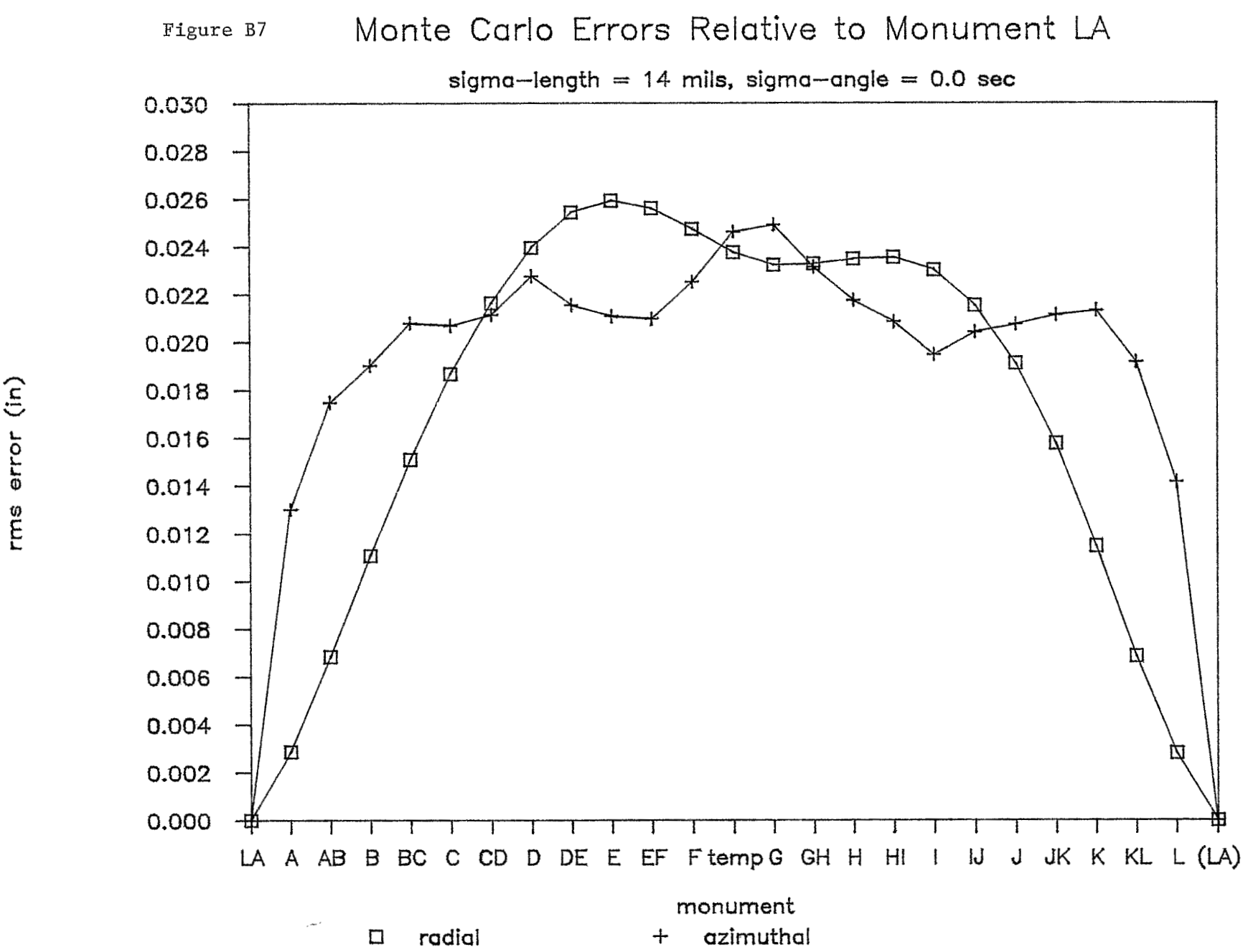
Monte Carlo Errors Relative to Monument LA
sigma–length = 14 mils, sigma–angle = 0.0 sec
rms error (in)
0.030
0.028
0.026
0.024
0.022
0.020
0.018
0.016
0.014
0.012
0.010
0.008
0.006
0.004
0.002
0.000
LA A AB B BC C CD D DE E EF F temp G GH H HI I IJ J JK K KL L (LA)
monument
radial
azimuthal

Figure B8

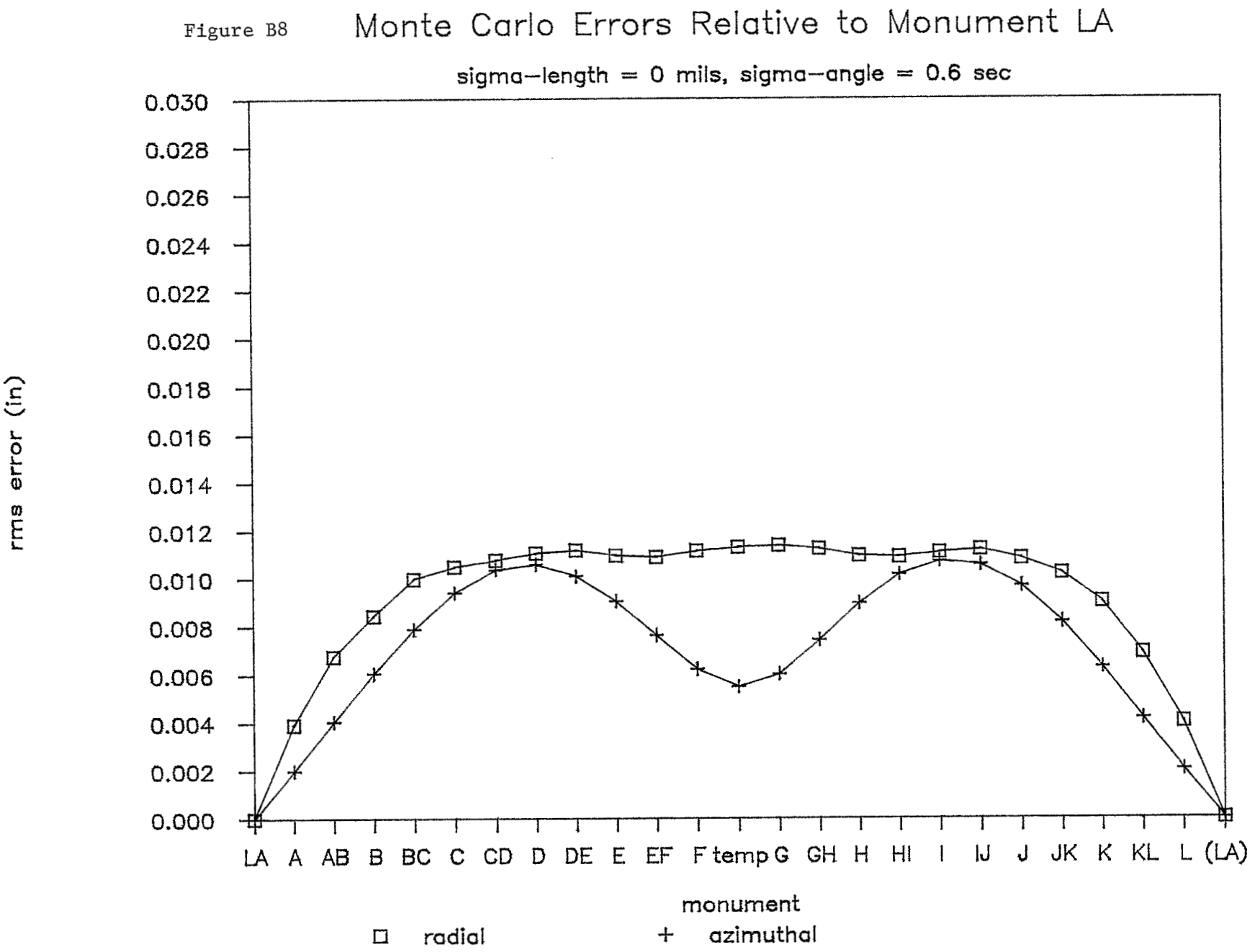
Monte Carlo Errors Relative to Monument LA
sigma–length = 0 mils, sigma–angle = 0.6 sec
rms error (in)
0.030
0.028
0.026
0.024
0.022
0.020
0.018
0.016
0.014
0.012
0.010
0.008
0.006
0.004
0.002
0.000
LA A AB B BC C CD D DE E EF F temp G GH H HI I IJ J JK K KL L (LA)
monument
radial
azimuthal

Figure B9

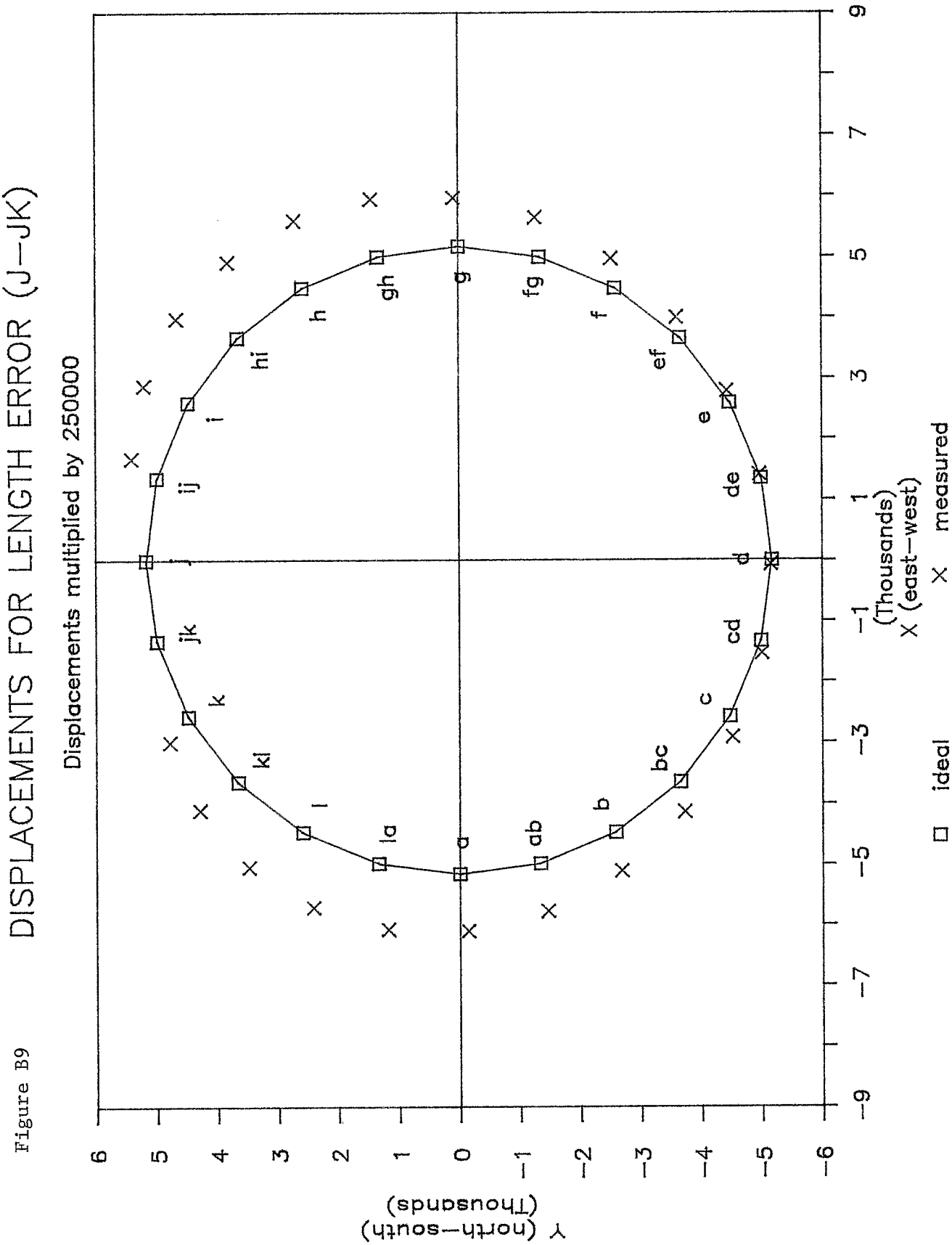
DISPLACEMENTS FOR LENGTH ERROR (J–JK)
Displacements multiplied by 250000
Y (north–south)
(Thousands)
X (east–west)
ideal
measured

Figure B10

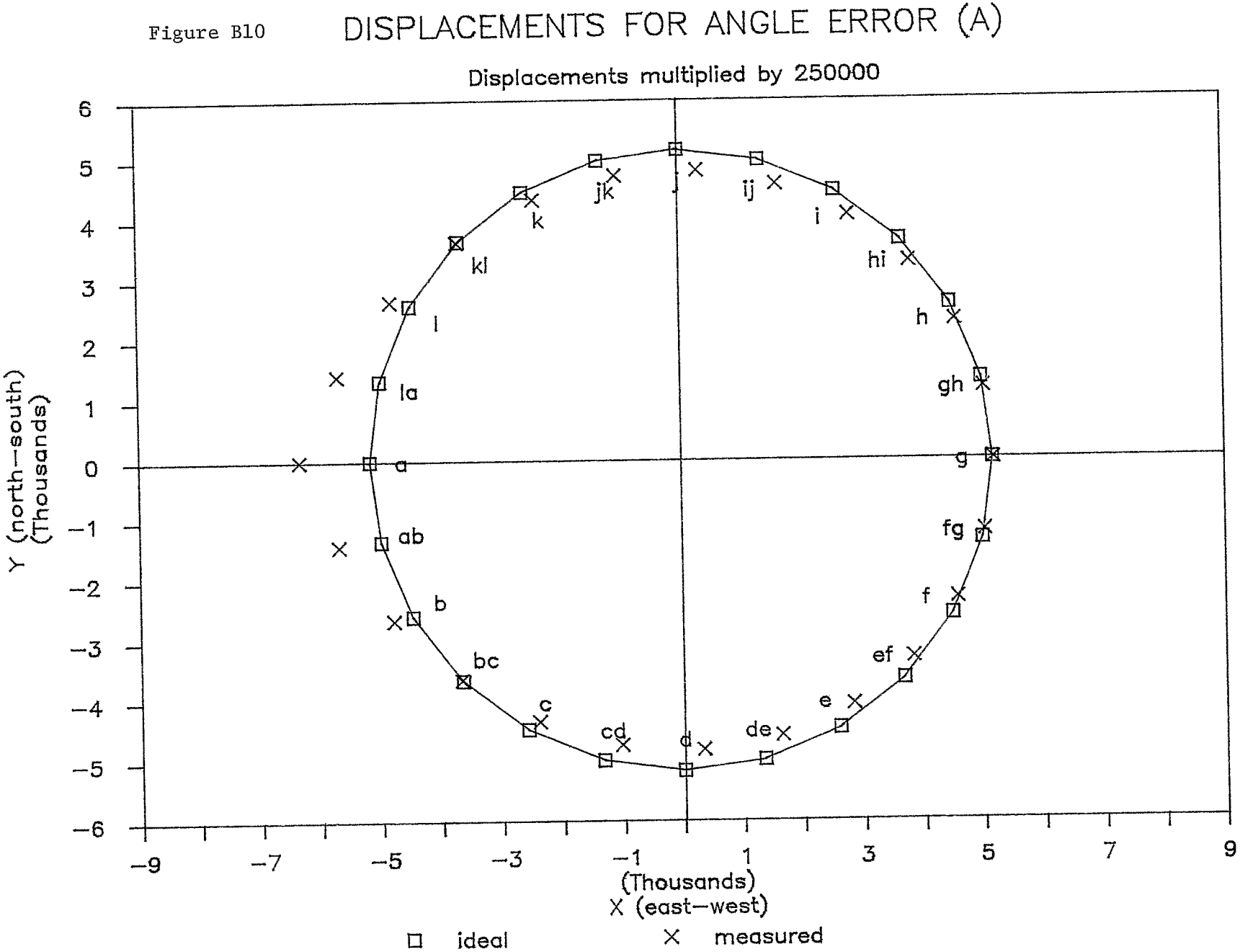
DISPLACEMENTS FOR ANGLE ERROR (A)
Displacements multiplied by 250000
Y (north–south) (Thousands)
X (east–west) (Thousands)
ideal
measured
a
ab
b
bc
c
cd
d
de
e
ef
f
fg
g
gh
h
hi
i
ij
j
jk
k
kl
l
la

Figure B11

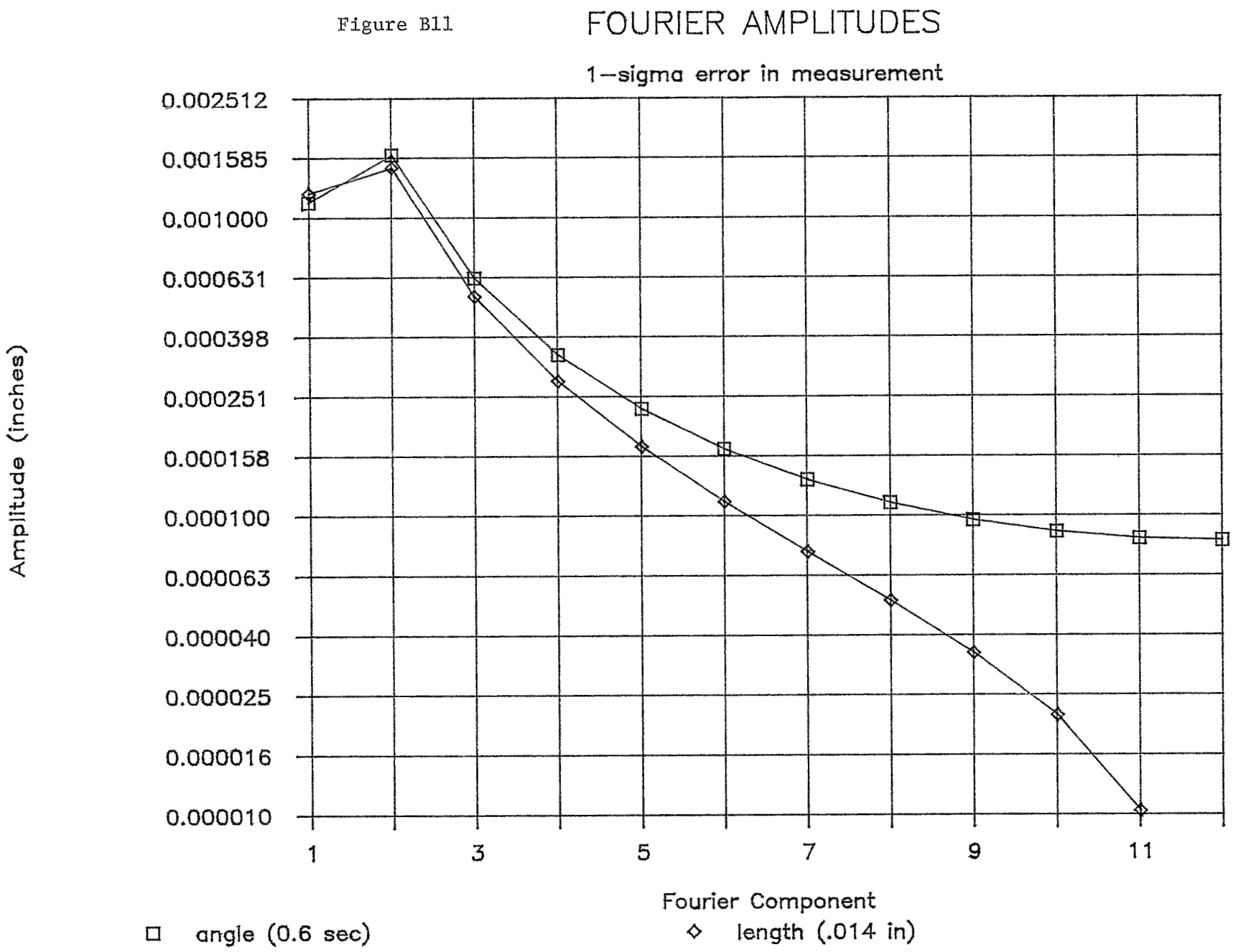
FOURIER AMPLITUDES
1—sigma error in measurement
0.002512
0.001585
0.001000
0.000631
0.000398
0.000251
0.000158
0.000100
0.000063
0.000040
0.000025
0.000016
0.000010
Amplitude (inches)
1
3
5
7
9
11
Fourier Component
angle (0.6 sec)
length (.014 in)

Figure B12

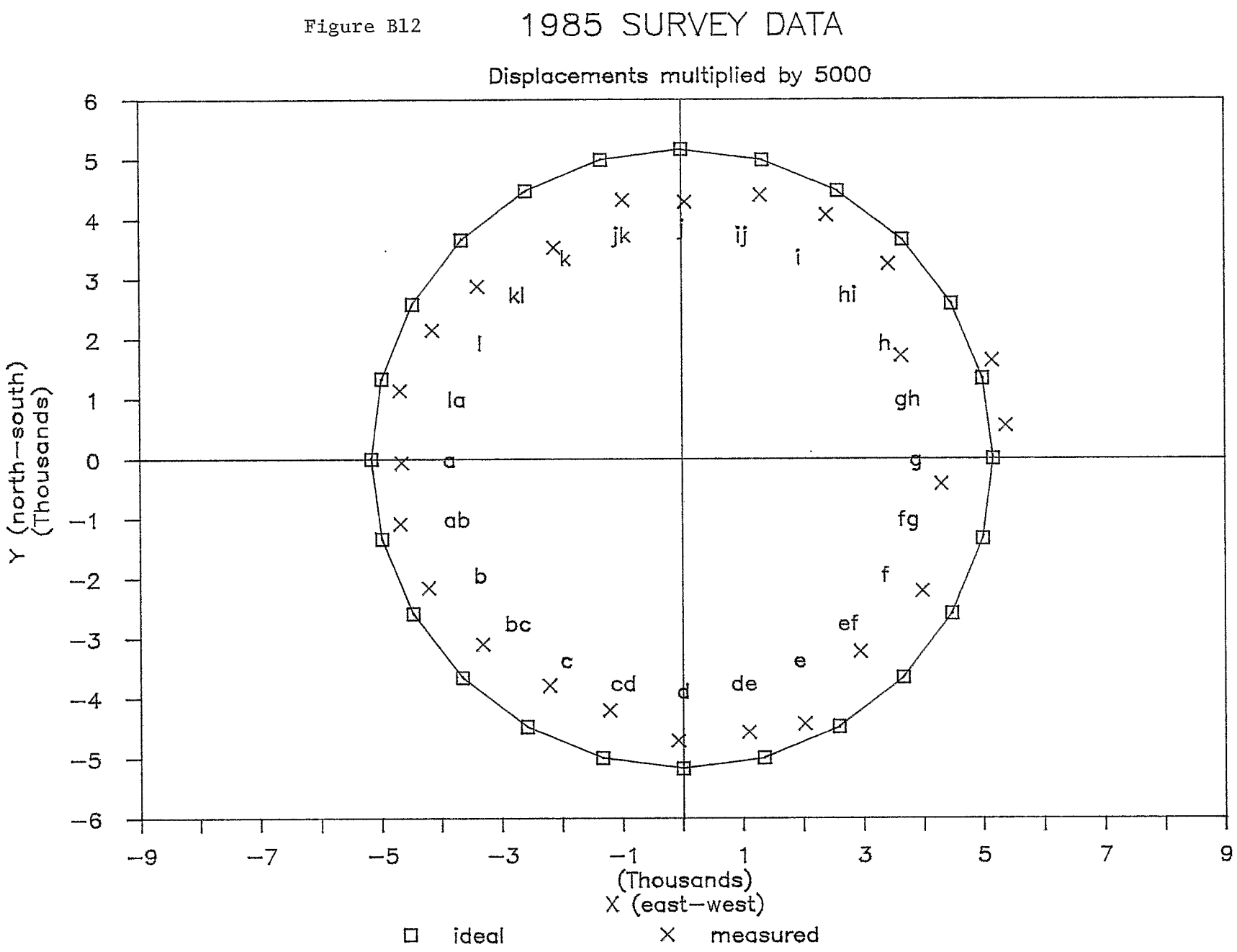
1985 SURVEY DATA
Displacements multiplied by 5000
Y (north–south) (Thousands)
X (east–west) (Thousands)
ideal
measured
jk
ij
i
k
kl
hi
l
h
la
gh
a
g
ab
fg
b
f
bc
ef
c
e
cd
de
d